3rd China-Japan Joint Workshop on Positron Science (JWPS2017)
JJAP Conf. Proc. **7**, 011203 (2018) https://doi.org/10.7567/JJAPCP.7.011203

Aging Induced Enhancement of Pore Interconnectivity of Porous Silica Investigated by Nitrogen Adsorption and Cyclic Voltammetry

Xiaoyu He[1], Bangyun Xiong[2], Lei Liu[1], Xiaonan Wang[1], Chunqing He[1]*

[1]*Key Laboratory of Nuclear Solid State Physics Hubei Province, School of Physics and Technology, Wuhan University, Wuhan 430072, China*
[2]*School of Materials Science and Energy Engineering, Foshan University, Foshan 528000, China*

E-mail: hecq@whu.edu.cn

(Received October 23, 2017)

Pore interconnectivities of mesoporous silica prepared with precursor sols aged for various times were investigated by N_2 adsorption-desorption measurement and cyclic voltammetry. With increasing aging time of the precursor sol to 4 days, an abnormal decrease in both total open volumes and specific surface areas was found. However, with further increasing the aging time to 15 days, the total open volumes and specific surface areas dramatically increased, indicative of the formation of highly interconnected pores and a remarkable increase in the silica porosity. This was further confirmed by cyclic voltammetry measurements using aqueous potassium iodide solutions on the corresponding silica films, which showed a significant rise in redox current and total charge Q across the films prepared after a longer time aging of precursor sols. This rise can be attributed to the diffusion of I^- across the silica films with enhanced pore interconnectivity, despite of the decline in total porosity for some silica samples.

1. Introduction

Because of their tunable pore size, high specific surface area and porosity, and good chemical and thermal stability, mesoporous silica has been suggested as a promising material for catalysts [1], drug delivery [2, 3], separation and adsorption [4], optical and electrical materials, and hydrogen storage [5, 6]. Applications of silica materials are closely associated with their mesostructures. For instance, an ordered mesoporous structure with connected channels is key to enhance the conversion efficiency of optical and electrical materials, and is also efficient to improve the rate capability of lithium ion batteries. Thus, it is meaningful to explore the conditions influencing pore interconnectivity and porosity of mesoporous silicas. Generally speaking, a number of preparation conditions, such as the synthetic method [7], surfactant content [8–10], pH [11], post-treatments [12] and sol aging time [13–18], etc., have been found to influence the mesostructure of silicas. Besides, various techniques for characterization of structures of pores are important and should be noted [19–22]. It is well known that the N_2 adsorption-desorption measurement is one of the most convenient techniques to characterize mesostructures [23, 24]. Nitrogen adsorption isotherms can be used to determine specific surface area, pore volume and pore size distribution, and might also reveal pore connectivity. Recently, ion diffusion in porous silica was used to study pore connectivity of mesoporous silica films [8].

In this work, precursor sol-aging induced enhancement of pore interconnectivity of porous silica prepared with a triblock copolymer has been studied by N_2 adsorption-desorption and cyclic voltammetry.

2. Experimental

2.1 Materials and sample preparation

Mesopore silica powders and films were synthesized with triblock copolymer F88 (BASF surfactant, EO100PO39EO100, M_w = 11400 g mol^{-1}) as the structure-directing agent and tetraethoxysilane (TEOS) as the network precursor. The process was executed in a similar way as previously reported [13]. Firstly, silica sol was prepared with precursors of TEOS (11.92 ml), EtOH (74.85 ml) and 0.02 mol L^{-1} dilute HCl (7.68 ml) stirred at 70 °C for 1 hour. The resulting solution was stirred for 1 hour at room temperature with the addition of triblock copolymer solution (3.84 g F88 and 18 ml EtOH). Finally, transparent silica sol was obtained. The final molar ratio was 1 TEOS ∶ 29.91663 C_2H_5OH: 8 H_2O: 0.00288 HCl: 0.00633 F88 in the sol. The precursor solution was separated into four parts, which were stored in sealed containers and aged for various durations at room temperature, i.e. 1 day, 4 days, 8 days and 15 days, respectively, from which the prepared samples were denoted as sample 1d, 4d, 8d and 15d. Silica powders were obtained after the sols were dried at 100 °C for 3 hours in vacuum, and then calcined at 450 °C for 5 hours in a tube furnace in air to remove the structure-directing agent. Meanwhile, silica films were spin-coated on polished (100) silicon wafers and indium tin oxide (ITO) slides with various aging times, respectively. The spin-coating was achieved at a beginning speed of 750 rpm for 3 s and a subsequent rate of 1250 rpm for 7 s. The deposited silica films were dried at 100 °C for 30 minutes in vacuum and then calcined at 450 °C for 5 hours in a tube furnace in air.

2.2 Characterization

Nitrogen adsorption-desorption measurements were implemented using a static nitrogen adsorption instrument (JW-BK122W) to investigate the pore size distribution, total pore volume and specific surface area. Prior to the measurements, the silica powders were preheated at 130 °C in vacuum for 3 hours. An electrochemical workstation (CS310, Correst) with a traditional three-electrode cell was employed for cyclic voltammetry measurements. After removing the surfactant F88 by calcination, porous silica films/ITO electrodes were treated as working electrodes. The electrolyte solutions were loaded in Teflon reservoirs fastened on the surfaces of the working electrodes. The counter electrode and reference electrode were composed of Pt wire electrode and saturated calomel electrode (SCE), respectively. Cyclic voltammetry curves were collected from −0.6 V to 1.6 V for mesoporous silica films prepared from the sols aged to various times. The refractive indices of the porous silica films, deposited on polished (100) silicon wafers, were measured by ellipsometry under flowing N_2 gas.

3. Results and discussions

3.1 N_2 adsorption-desorption measurements for silica powders

The influence of the precursor the solution aging time on the mesostructure of silica powders, prepared with triblock copolymer F88, was investigated by N_2 adsorption-desorption. The N_2 adsorption isotherms are shown in Fig. 1(a). It can be seen that all samples show a type IV isotherm and a classical H_2-type hysteresis loop defined by IUPAC, indicative of cage-like mesopores with window pore sizes smaller than 4 nm. The volume of condensed N_2 adsorbed in the silica powder samples shows a decrease with the precursor sols aged from 1 day to 4 days. In contrast, a continuous increase in the total volume of condensed N_2 is found after the precursor sol is aged over 4 days. The capillary condensation step occurs around the relative pressure from 0.4 to 0.6, from which mesopore size distributions are calculated based on the Barrett-Joyner-Halenda (BJH) method. As shown in Fig. 1(b), pore distributions seem to be essentially the same for the samples prepared after aging from 1 day to 4 days, much longer aging times resulted in smaller pore sizes with a relatively wider distribution.

From the N_2 adsorption isotherms, pore sizes, specific surface areas and total open pore volumes in silica powders were calculated and are listed in Table 1. It was found that total pore volume and

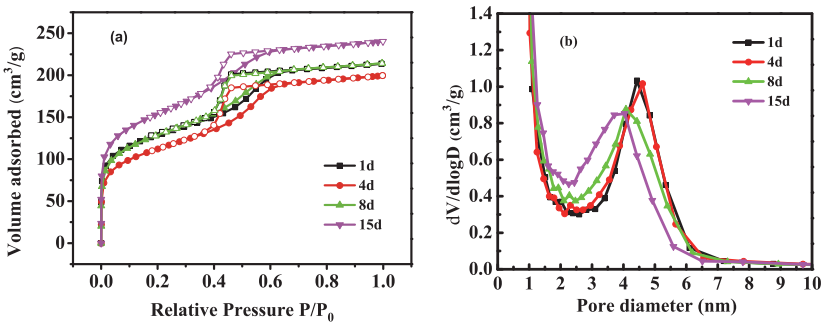

Fig. 1 (a) N_2 adsorption isotherms (Solid and open symbols are represented for adsorption and desorption branches, respectively) and (b) pore diameter distributions of mesoporous silicas from precursor sols aged for different times.

Table I The properties of mesoporous silicas templated by triblock copolymer F88.

Samples	Cage pore size [nm]	Window pore size [nm][a]	BET surface areas [$m^2\,g^{-1}$]	Total pore volume [$cm^3\,g^{-1}$][b]
1d	4.43	3.40	446	0.256
4d	4.61	3.40	390	0.242
8d	4.08	3.41	449	0.278
15d	4.04	3.13	538	0.300

[a]The window pore size is calculated from the desorption branch.
[b]The total pore volume is estimated based on the volume adsorbed at $p/p_0 \sim 0.993$.

Brunauer-Emmett-Teller (BET) specific surface areas drop from 0.256 $cm^3\,g^{-1}$ and 446 $m^2\,g^{-1}$ to 0.242 $cm^3\,g^{-1}$ and 390 $m^2\,g^{-1}$ for sample 1d and 4d, respectively, which may be caused by the change of pore morphology at a short sol aging time. With further increasing the aging time from 4 days to 15 days, however, both of values show a gradual increment. These results suggest that more isolated pores may coalesce into interconnected pores in silica powders with further prolonging the aging time. The increase in total pore volume and specific surface areas indicates that open porosity is enhanced in silicas. Simultaneously, the mesopore size, calculated from the adsorption branch, shows a further decrement from 4.61 nm to 4.04 nm for longer aging times. It is worth noting that the cage pore size seems not to depend on the aging time if the aging time of the precursor sol is beyond 8 days. This suggests that the average pore size in silica is no longer influenced given the long enough aging time, which is in agreement with the results of previous research [13]. Furthermore, the wider pore size distribution with the decrement of cage pore diameter may contribute to the enhancement of open porosity after the precursor sol is aged for a longer time. The results of nitrogen adsorption isotherms reveal a strong dependence of the mesostructures of silicas on the precursor sol aging time, and highly interconnected pores may be formed in silica powders with a long precursor sol aging time. In order to further demonstrate the variation of mesostructure in silica materials, ion transportation in silica films was investigated by cyclic voltammetry.

3.2 Ellipsometry and cyclic voltammetry for silica films

According to the mean field approximation, the refractive index of a porous silica films is determined by the intrinsic refractive index of pores ($n = 1$) in the silica film and that of the silica skeleton. Thus, apparent porosity (pore volume fraction V_p) of the mesoporous silica films can be evaluated based on

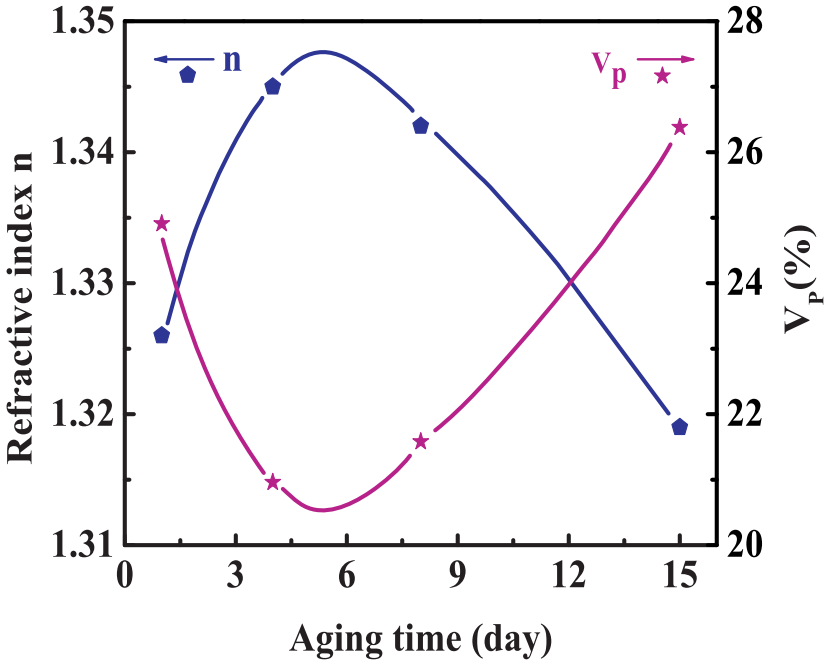

Fig. 2 Variations of refractive index and porosity as a function of aging time.

the refractive indices according to Lorentz-Lorenz equation [25], which can be expressed as

$$\frac{n_f^2 - 1}{n_f^2 + 2} = \left(1 - V_p\right) \frac{n_s^2 - 1}{n_s^2 + 2} \tag{1}$$

where n_f and n_s are the index of refraction of the silica film and that of silica skeleton, respectively. The value for amorphous nonporous silica (1.45) is applied to n_s in Lorentz-Lorenz equation. Fig. 2 shows the apparent porosities and refractive indices of the silica films as a function of aging time for the precursor sols. It can be seen that the refractive index of the films increased from 1.326 to 1.345 with increasing the precursor sol aging time from 1 day to 4 days. However, the refractive index shows a continuous decrease with additional aging time, showing a maximum around the 4-day-aged sample. On the contrary, the porosity decreases from 24.91 % to 20.95 % after 4 days of aging. With prolonging the aging time, a large increase in the porosity is observed. These changes in refractive indices and porosities is in agreement with the results of N_2 adsorption-desorption measurements, suggesting the pore morphology changes after aging for around 4 days. Furthermore, a high porosity is found for the longest aged film (15d), which is consistent with its high specific surface area (538 $m^2\,g^{-1}$) and large total pore volume obtained from the result of BET. The high porosity and wider pore size distribution suggests the coalescence of isolated pores to interconnected ones occurs at a longer aging time of the precursor sol.

Our previous work has shown that electrochemical cyclic voltammetry can be used as a new approach to explore the interconnectivity of mesopores in porous films by measuring the ion diffusion across them [8]. Cyclic voltammetry curves were collected with potassium iodide (KI) solution with the addition of potassium biphthalate (pH = 4.1) as the buffering agent. Figure 3 displays the curves of cyclic voltammetry for silica films deposited on ITO slides. It can be seen that the current intensity for anodic peak of I^-/I_2 on silica film/ITO electrode shows a stable increment with increasing in aging time. For the film 1d, a rather weak response on silica films/ITO electrodes for redox probe I^-/I_2 is attributed to the low interconnectivity of the pores in silica film. The anodic peak apparently increases with prolonging aging time. The current intensity for the film 15d is much higher than other

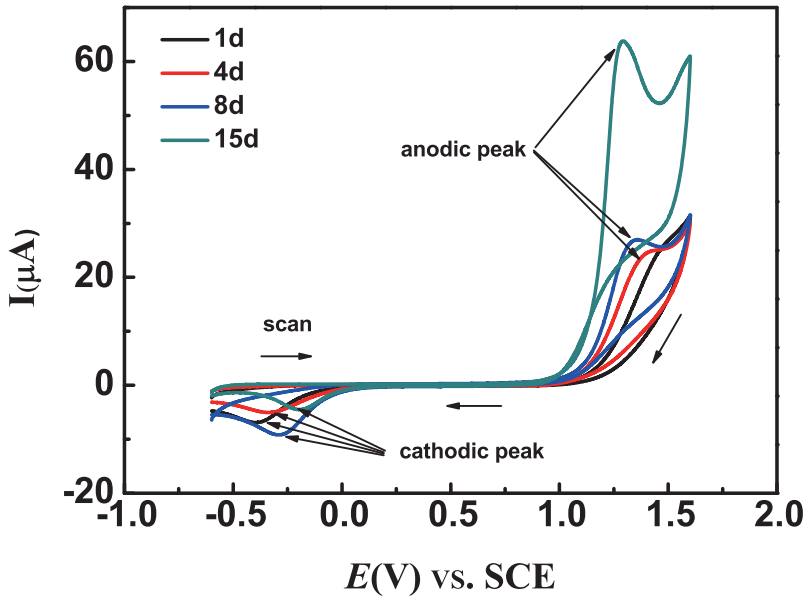

Fig. 3 Cyclic voltammetry curves for silica films/ITO electrodes prepared by surfactant F88 after different aging durations at a scanning rate of 10 mV s^{-1}.

film samples, which is due to the significant enhancement in pore connectivity and porosity. It should be noted that anodic peak shows a sharp increase in the current intensity at increasing voltage, rising more sharply for the film 15d in comparison with that of the film 8d. Again, this strongly indicates the interconnectivity of pores in silica films becomes much higher with longer aging time. The highly interconnected pores allow the I^- anions to diffuse across the silica films, they can then be oxidized on the surface of ITO electrodes leading to a strong redox signal. In addition, with increasing aging time, the cathodic peaks shift from −0.19 V to −0.40 V and the anodic peaks shift in a positive direction (1.29 V to 1.44 V) for silica film/ITO electrodes. This effect may be caused by a change in the isoelectric point due to the adsorption of I^-/I_2 in the micropores near the surface of the silica films with various porosities.

The total charge Q, due to oxidization for I^- on the surface of silica/ITO electrodes, is obtained by integration from the anodic peaks in cyclic voltammetry curves. Q is calculated as follows:

$$Q = \int i\,\mathrm{d}t = \int \frac{i\mathrm{d}E}{\nu} \tag{2}$$

where i and E are the electric current and voltage, respectively, and ν is the scanning rate (10 mV s^{-1}).

Fig. 4 shows the variation of the total charge Q as a function of precursor sol aging time. It is interesting to find that Q continuously rises with increasing of aging time. A slow increase of Q is seen for aging times less than 8 days, while a dramatic increase of Q is found for 15 days of aging, which is attributed to the formation of highly interconnected pores with high open porosity in silica film 15d. Hence, the current intensity and total charge Q for anodic peaks due to I^- diffusion across the silica films directly confirmed that the interconnectivities of pores in silica films are enhanced with increased aging time of the precursor sol. This result further revealed that some isolated pores coalesced into interconnected pores, even when the total porosity declined for the silicas prepared after the precursor sols were aged no longer than 8 days.

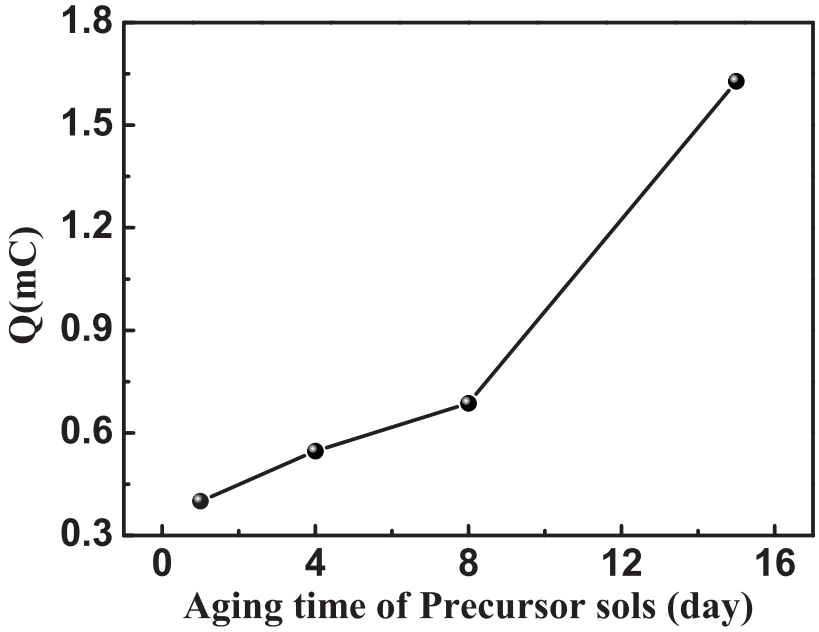

Fig. 4 The relationship between the total charge Q and precursor sols aging time.

4. Conclusion

In summary, N_2 adsorption-desorption measurement and cyclic voltammetry have been utilized to study the pore interconnectivity of porous silica prepared by surfactant F88 as a function of sol-aging time. The results from N_2 adsorption isotherms showed that the total volume of condensed N_2 and in particular the specific surface areas in porous silica decreased after the precursor sol was aged for up to 4 days. However, these quantities increased continuously with further aging. These results indicated that pore morphology may be changed in silica around an aging time of 4 days, and that pore interconnectivity and porosity of silica powders increase significantly with a longer aging times of the precursor sol. This was further confirmed by ellipsometry on silica films, which demonstrated that the apparent porosity varied in a similar way as the total volume of adsorbed N_2. Cyclic voltammetry showed that the total charge of anodic peak due to I^- diffusion across the film increased gradually with the sol aging up tp 8 days, and it showed a much larger increase with an increased sol aging time of 15 days. These results further demonstrated that pore interconnectivity could be enhanced significantly given a longer aging time of the precursor sol due to the coalescence of isolated pores during the process of self-assembly.

Acknowledgment

This work was supported by the National Science Foundation of China (NSFC) under Grant Nos. 11575130 and 11705029.

References

[1] Y. Zhang, E. C. Judkins, D. R. McMillin, D. Mehta, and T. Ren, ACS. Catal. **3**, 2474 (2013).
[2] S. Saha, K. C.-F. Leung, T. D. Nguyen, J. F. Stoddart, and J. I. Zink, Adv. Funct. Mater. **17**, 685 (2007).
[3] H. Bao, J. Yang, Y. Huang, Z. P. Xu, N. Hao, Z. Wu, G. Q. Lu, and D. Zhao, Nanoscale **3**, 4069 (2011).
[4] M. O. Adebajo, R. L. Frost, J. T. Kloprogge, O. Carmody, and S. Kokot, J. Porous Mat. **10**, 159 (2003).
[5] P. Yang, D. Zhao, D. I. Margolese, B. F. Chmelka, and G. D. Stucky, Chem. Mat. **11**, 2813 (1999).
[6] V. C. Menon and S. Komarneni, J. Porous Mat. **5**, 43 (1998).

[7] J. Brown, R. Richer, and L. Mercier, Microporous Mesoporous Mat. **37**, 41 (2000).
[8] X. Tang, B. Xiong, Q. Li, W. Mao, W. Xiao, P. Fang, and C. He, Electrochim. Acta. **168**, 365 (2015).
[9] B. Xiong, W. Mao, X. Tang, C. He, J. Appl. Phys. **115**, 094303 (2014).
[10] C. He, T. Oka, Y. Kobayashi, N. Oshima, T. Ohdaira, A. Kinomura, R. Suzuki, Appl. Surf. Sci. **255**, 183 (2008).
[11] R. Zaleski, M. Gorgol, A. Kierys, and J. Goworek, Adsorption **22**, 745 (2016).
[12] H. J. Shin, R. Ryoo, M. Kruk, and M. Jaroniec, Chem. Commun. **349** (2001).
[13] C. He, M. Muramatsu, N. Oshima, T. Ohdaira, A. Kinomura, and R. Suzuki, Phys. Lett. A. **355**, 73 (2006).
[14] X. Zhang, W. Wu, J. Wang, and C. Liu, Thin Solid Films **515**, 8376 (2007).
[15] C. McDonagh, F. Sheridan, T. Butler, and B. D. MacCraith, J. Non-Cryst. Solids **194**, 72 (1996).
[16] S.-B. Jung and H.-H. Park, Thin Solid Films **494**, 320 (2006).
[17] C. He, R. Suzuki, T. Ohdaira, N. Oshima, A. Kinomura, M. Muramatsu, and Y. Kobayashi, J. Chem. Phys. **331**, 213 (2007).
[18] J. R. Matos, M. Kruk, L. P. Mercuri, M. Jaroniec, L. Zhao, T. Kamiyama, O. Terasaki, T. J. Pinnavaia, and Y. Liu, J. Am. Chem. Soc. **125**, 821 (2003).
[19] B. Xiong, W. Mao, J. Yue, X. Xu, and C. He, Phys. Lett. A **378**, 249 (2014).
[20] M. Klingstedt, K. Miyasaka, K. Kimura, D. Gu, Y. Wan, D. Zhao, and O. Terasaki, J. Mater. Chem. **21**, 13664 (2011).
[21] A. Walcarius and A. Kuhn, Trac-Trends Anal. Chem. **27**, 593 (2008).
[22] G. A. Mabbott, J. Chem. Educ. **60**, 697 (1983).
[23] K. S. W. Sing, J. Porous Mat. **2**, 5 (1995).
[24] K. S. W. Sing, D. H. Everett, R. A. W. Haul, L. Moscou, R. A. Pierotti, J. Rouquérol, and T. Siemieniewska, Pure Appl. Chem. **57**, 603 (1985).
[25] P. Revol, D. Perret, F. Bertin, F. Fusalba, V. Rouessac, A. Chabli, G. Passemard, and A. Ayral, J. Porous Mat. **12**, 113 (2005).